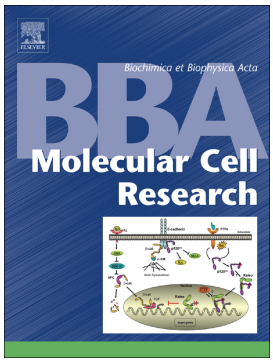

Ageing modulates human dermal fibroblast contractility: quantification using nano-biomechanical testing

Zhuonan Yu, Matthew J. Smith, Richard C.M. Siow, Kuo-Kang Liu

PII: S0167-4889(21)00026-4

DOI: https://doi.org/10.1016/j.bbamcr.2021.118972

Reference: BBAMCR 118972

To appear in: *BBA - Molecular Cell Research*

Received date: 20 November 2020

Revised date: 19 January 2021

Accepted date: 24 January 2021

Please cite this article as: Z. Yu, M.J. Smith, R.C.M. Siow, et al., Ageing modulates human dermal fibroblast contractility: quantification using nano-biomechanical testing, *BBA - Molecular Cell Research* (2021), https://doi.org/10.1016/j.bbamcr.2021.118972

Ageing modulates human dermal fibroblast contractility: quantification using nano-biomechanical testing

Zhuonan Yu[1+], Matthew J. Smith[2+], Richard C. M. Siow[2]*, Kuo-Kang Liu[1]*

[1]School of Engineering, University of Warwick, Coventry, United Kingdom

[2]School of Cardiovascular Medicine & Sciences, King's British Heart Foundation Centre of Research Excellence, Faculty of Life Sciences and Medicine, King's College London, London, United Kingdom

[+] Z.Y. & M.J.S are joint first authors

* R.C.M.S & K.K.L are joint senior authors

Address correspondence to K. K. Liu, University of Warwick, School of Engineering, Coventry, United Kingdom.

Telephone: +44(0)2476574348 Electronic mail: i.k.liu@warwick.ac.uk

Abstract

Dermal fibroblasts play a key role in maintaining homoeostasis and functionality of the skin. Their contractility plays a role in changes observed during ageing, especially in processes such as wound healing, inflammation, wrinkling and scar tissue formation as well as structural changes on extracellular matrix. Although alternations in skin physiology and morphology have been previously described, there remains a paucity of information about the influence of chronological ageing on dermal fibroblast contractility. In this study, we applied a novel nano-biomechanical technique on cell-embedded collagen hydrogels in combination with mathematical modelling and numerical simulation to measure contraction forces of normal human dermal fibroblasts (NHDF). We achieved quantitative differentiation of the contractility of cells derived from 'young' (< 30 years old) and 'aged' (> 60 years old) donors. Transforming growth factor β1 (TGF-β1) was used to stimulate the fibroblasts to assess their contractile potential. NHDF from aged donors exhibited a greater basal contractile force, while in contrast, NHDF from young donors have shown a significantly larger contractile force in response to TGF-β1 treatment. These findings validate our nano-biomechanical measurement technique and provide new insights for considering NHDF contractility in regenerative medicine and as a biomarker of dermal ageing processes.

Keywords: Cell Mechanics; Collagen Hydrogel; Nano-indentation; Force-displacement Measurement; TGF-β1; Finite Element

1. INTRODUCTION

Ageing is associated with progressive degradation of optimal function, metabolic efficiency and adaptation to environmental stresses, leading to cellular, structural and biomechanical alterations at both molecular and tissue levels [1, 2]. Skin is the most extensive tissue of the human body, acting as an interface with the external environment, maintaining homeostasis, defending against pathogens and harmful electromagnetic radiations [3].

The skin has a layered structure, with each layer serving a distinct purpose in the function of the skin, of which dermis serves a major role. The dermis mainly consists of extracellular matrix (ECM) and provides the majority of structural and mechanical strength to the skin. Fibroblasts play a vital part in the remodelling and sustaining the homeostasis of the ECM by producing and disintegrating its components such as collagen, elastin and glycosaminoglycans (GAGs) [4]. Dermal fibroblasts are also critical to the wound healing process through their proliferation, migration and the ability to respond to cytokines such as transforming growth factor beta (TGF-β) for myofibroblast differentiation and contraction [5]. Dermal fibroblasts rarely regenerate due to their post-mitotic nature, thus accumulate damages and adapt to environmental stresses associated with extrinsic ageing [6].

In biomolecular terms, ageing of dermal fibroblasts can lead to DNA damage at telomeres [7], a decline in proteasome activities [8], decreased antioxidant defences and insensitivity to growth factors. From a morphological and biomechanical perspective, alterations in cell size and volume [9], increase in stiffness, reduction in mobility and plasticity have been reported [9, 10]. However, there remains a paucity of information on how contractility and ageing relate, though being an important parameter in cellular biomechanics. Dermal fibroblasts contraction is closely related to physiological processes such as wound healing,

wrinkling, response to inflammation, angiogenesis and metastasis [11, 12]. Thus, investigating the changes in contractility of dermal fibroblasts will provide novel insights for skin ageing from biomechanical perspectives and clinical applications of monitoring the impact of ageing.

Several techniques have been developed for *in vitro* studies of cell contraction, which can be briefly categorised based on whether contraction force is measured on a single cell basis or populations of cells. Traction force microscopy (TFM) and elastic micro-pillar (EMP) technique are two well-known single-cell-based approaches [13]. They share the working principle of measuring the deformation of the substrate with known elasticity due to cell contraction. TFM utilises cells cultured on the surface of a two-dimensional (2D) substrate and tracks substrate deformation through displacements of embedded fluorescent microbeads. EMP requires cells to be placed on the tips of microfabricated elastomeric beam array, which degree of pillar deflection will reflect the magnitude of contraction force. Both techniques are highly quantitative yet inherently neither cell-friendly nor physiological as the contraction is assessed on a 2D surface instead of a three-dimensional (3D) biomimetic matrix. Recently developed 3D-TFM technique embeds both cells and beads into a deformable matrix and tracks bead movements in 3D with confocal microscopy and optical coherence microscopy [14, 15]. However, such a technique still has shortfalls in resembling *in vivo* conditions as the cell seeding density is usually kept at a very low level to avoid interferences between traction fields of cells, which may hinder their mechanosensing process.

Techniques for contraction force measurement in populations of cells can mostly provide cells with a biomimetic environment. Among these, collagen gel contraction assay (CGCA) is

the most prevailing technique as collagen is a key component of the ECM that facilitates cell contraction. CGCA provides cells with a physiologically relevant 3D matrix environment, which also encourages cell contraction through mechanosensing. Embedded cells induce a progressive contraction of the gel, resulting in the reduction of the diameter of disk-shaped gel [16]. Contractility is commonly assessed by comparing images of the gel taken at the beginning and the end of a contraction period. However, it can lead to error as the changes in the gel's thickness and stiffness during contraction were not considered. To improve the quantitativeness of the CGCA technique, culture force monitor (CFM) technique was developed by attaching strain gauges on the edge of cell-embedded collagen gel [17]. CFM achieves continuous and direct measurement of cellular contraction force without the influence of varying elasticity of collagen gel. However, the measurement is limited to uniaxial stress as the strain gauges are only capable of measuring contraction force in single directions. Moreover, the attachment of strain gauges to the gel unavoidably compromises cell-friendliness to some extent.

We have previously developed a novel technique, allowing quantitative assessment of cellular contraction force by accurate measurement of the elasticity of cell-embedded hydrogels through nano-indentation testing in combination with mathematical modelling [18]. The nano-biomechanical measurement technique based on 3D cell-embedded collagen hydrogel hence excels in cell-friendliness compared with TFM and EMP techniques. The technique also factors in contraction force in all directions with minimal disturbance to the cells, advantageous over CFM.

The vast majority of the studies aimed at characterising behavioural change of dermal fibroblasts during ageing have adopted '*in vitro*' models, which have used early and late

passage cells as a surrogate for young and aged cells respectively [12]. Such models have yielded insights into the ageing process, however, do not accurately recapitulate chronological ageing and cannot replace studies using cells isolated from young and aged human donors [2], especially in the light of complex ageing mechanisms in the skin arising from both intrinsic physiological and extrinsic environment-related ageing. Employing our novel nano-biomechanical technique, we have studied the contractility of cultured NHDF. The present study investigates the influence of ageing to the contractility of NHDF isolated from the skin of young and aged donors by accurately measure the contraction force generated. Our results provide new insights into the baseline contractility of cells from both young and aged individuals, as well as showing the potential decline in responsiveness to human TGF-β1 by the aged NHDF. We demonstrate that our novel technique can differentiate and quantify the altered contractility between the young and aged dermal fibroblasts.

2. MATERIALS AND METHODS

2.1 Cell Culture and Preparation for Seeding

NHDF cell lines derived from skin biopsies on healthy female individuals with respective age of 20, 26, 29, 62, 68 and 75 were purchased from commercial sources; Caltag Medsystems (Buckingham, UK), Axol Bioscience (Cambridge, UK) and Lonza (Basel, Switzerland). Cells were expanded in low glucose phenol red-free Dulbecco's modified Eagle's medium (DMEM) (Merk, USA) with 10% foetal bovine serum (FBS) (Merk, USA), 2 mM L-glutamine and 1% penicillin/streptomycin at 5% CO_2 and 37 ℃. For all experiments, cells between passage 3 to

5 were used. For comparing contractility at a different age, cell lines were grouped into 'young' (<30 years old) and 'aged' (>60 years old) groups resulting in 3 donors per group.

2.2 Cell-embedded Collagen Hydrogel Preparation

NHDF were washed with PBS and exposed to 0.05% Trypsin/EDTA for 4 minutes and detached from the bottom of culture flasks, quenched with complete media, centrifuged at 1,000 rpm for 5 minutes, re-suspended with PBS and counted on a haemocytometer.

Hydrogels were made using rat-tail type I collagen (Corning, USA). All materials were kept on ice to avoid premature collagen polymerisation. A hydrogel solution was first made containing 1-part DMEM (10x) (Sigma, USA) and 8-parts collagen with double distilled water. This solution was then neutralised with NaOH solution before adding 1-part cell suspension in the PBS to give a final collagen concentration of 1.5 mg ml^{-1}. The solution was then transferred into non-culture-coated Petri dishes of 35 mm diameter (Corning, USA) (1.5 ml per dish) and allowed to polymerise in an air incubator at 37 ℃ for 30 minutes. Subsequently, 2 ml DMEM containing 1% FBS was added to each dish and then transferred to 5% CO_2 incubators at 37 ℃ for a further polymerisation and swelling of 90 minutes. Some dishes were stimulated with the agonist recombinant human TGF-β1 (eBioscience, UK), supplemented into the DMEM at the concentration of 5 ng ml^{-1} [19, 20]. Gels were dislodged from the bottom of the Petri-dish with a sterile spatula and suspended in the culture medium, allowing the free contraction of the gel for a further 48 hours. In order to assess the most suitable cell seeding density to measure the cell-embedded gel contraction, densities of 50,000; 100,000 and 200,000 cells ml^{-1} were initially chosen for comparison.

Based on the preliminary results, the seeding density of 50,000 cells ml^{-1} was selected for further study.

2.3 Measuring Hydrogel Elasticity Using Depth-sensing Bio-nano-indentation Tester

A tailored bio-nano-indentation tester was constructed, as shown in Figure 1. The primary function of the tester is to measure the elasticity of the cell-embedded hydrogel based on the depth-sensing indentation technique. The system was assembled around an inverted optical microscope (TE-2000-S, Nikon), on which a motorised *x-y* axis stage (ProScan III, Prior Scientific) was mounted. The motorised *x-y* stage was incorporated with a temperature control plate with a 35 mm Petri-dish holder (Temp. Control. iBidi) to maintain a constant temperature during the test process. The force measurement is achieved through a force transducer (406A, Aurora Scientific Inc, Canada) with a cylindrical glass indenter, which has a diameter of 1 mm. The transducer was actuated by a *z*-axis (vertical) stage (UTS 100CC with ESP301 Motion Controller, Newport) to achieve the acquisition of force-displacement (*F-D*) data by recording the two variables simultaneously during the indentation. The system is jointly capable of providing force and displacement resolutions down to 10 nN and 100 nm, respectively. All instruments incorporated in the tester were placed on an anti-vibration table (AVT-702, Wentworth Laboratories Ltd) to reduce environmental influences.

Figure 1.

Disk-shaped collagen gels were indented at the rate of 40 μm s^{-1} for the entire thickness of the gel, during which, force and displacement data were simultaneously recorded. Collagen

gel was removed from the liquid medium and placed in a separate Petri-dish. Samples were kept at 37 ℃ to preserve the functionality of the embedded cells and structural integrity of the gels. Seven evenly spaced diametrical points on the gel were selected for the measurements to be representative to the entire sample. The thickness of the gel was obtained by the differences in the displacements measured between the top surface of the gel and the surface of the Petri-dish.

A CCD camera with a long focal lens (Edmund Industrial Optics, VZM 450) was used to capture the top-view images of the gel before and after the contraction (shown in Figure 2(a)). The camera was mounted vertically downwards on a fixation which was calibrated at the start of the experiment to ensure no parallax error for the image acquisition process. The contraction of cell-embedded gels can be observed, as shown in Figure 2(a) and 2(b). ImageJ program (National Institutes of Health, USA) was used to measure the original radius (r_1) and the radius after contraction (r_2) of the gel. The areas of the gel and the Petri-dish within the top-view image were determined by contrast thresholding and edge detection. As the diameter of the Petri-dish has a known value of 35 mm, the radius of the gel can be determined in relation to the dish diameter. The adaptation of such approach allows gel radius to be measured regardless of the lens magnification.

Figure 2.

2.4 Theoretical Analysis

The nature of the indentation test is a rigid cylindrical punch indenting a gel which is a flat, incompressible elastic substrate. Hydrogels are generally recognised as hyperelastic materials, which exhibit nonlinear elastic behaviours under large deformation. However, at very low strain, it is predominantly linearly elastic. Thus, we can correlate the modulus with

the first 10% of the *F-D* curve based on the following expression derived from the Hertz contract theory [21].

$$E^* = \frac{F}{2rD}, \#(1)$$

where E^* is the reduced modulus of the gel, *F* is the measured force on the force transducer, *D* is the displacement of the indenter in relative to the gel top surface, and *r* is the radius of the indenter tip. Also, the Hertz contact model described the reduced modulus in the contract of two elastic bodies as:

$$\frac{1}{E^*} = \frac{1-\nu_g^2}{E_g} + \frac{1-\nu_i^2}{E_i}, \#(2)$$

where *E* is the Young's modulus, and *v* is the Poisson's ratio of the contract bodies. The subscripts '*g*' and '*i*' denote the properties of the gel and indenter, respectively. As the hydrogel is modelled as an incompressible material (*i.e.*, Poisson's ratio *v*=0.5) and indenter is rigid compared with gel (*i.e.*, $E_i >> E_g$), equation (2) can be simplified as:

$$E^* = \frac{4E_g}{3}, \#(3)$$

Furthermore, the gel can exhibit up to 50% diameter reduction during the contraction, where nonlinear elastic behaviour manifests; therefore, the strain-dependent elasticity [22] is employed to describe the nonlinear behaviour:

$$E_g = E_o \cdot \frac{(1-\bar{\epsilon})^2}{\bar{\epsilon} - \bar{\epsilon}^2 + \left(\frac{\bar{\epsilon}^3}{3}\right)} = F \cdot \frac{3}{8rD} \cdot \frac{(1-\bar{\epsilon})^2}{\bar{\epsilon} - \bar{\epsilon}^2 + \left(\frac{\bar{\epsilon}^3}{3}\right)}, \#(4)$$

where $\overline{\epsilon} = D/h_o$ (see the definition of h_o later) is the engineering strain, and E_0 is Young's modulus of the gel at $\overline{\epsilon} \approx 0$ [18].

The overall cell contraction force can be calculated based on the measured material parameters such as Young's modulus of the gel and the geometrical change of the gel. Furthermore, the single-cell contraction force can be calculated as an average of overall contraction force using cell number.

$$F_{single} = \frac{F_{total}}{n} = \frac{\pi \cdot E_g \cdot (h_0 + h_1) \cdot (r_0 - r_1)}{n} \quad ,\#(5)$$

F_{single} and F_{total} are the single-cell and the total contraction forces, respectively, and n is the number of cells within the gel. h and r represent the thickness and radius of the gel, respectively with subscripts '*0*' and '*1*' denoting their values before and after contraction.

2.5 Finite-element Model for Nano-indentation

To validate the parameters used in the theoretical analysis, a 2D axisymmetric finite-element (FE) model was created using ABAQUS FEA (Dassault Systems, France). The model adopts the same geometry and material properties of the cylindrical glass indenter and the collagen hydrogel, and the 3D nature of the gel is simulated by applying the rotational symmetry. Thus, it is a close representation of the nano-indentation experiment. Poisson's ratio for the hydrogel was varied from 0.45 to 0.499 (limited by FE approach) to verify the assumption on Poisson's ration in the theoretical analysis. The simulated indentation was performed at 40 μm s^{-1} for up to 0.5 mm displacement (engineering strain = 0.25), which is also in line with the experimental study. The mesh density of the FE model was designed to increase with proximity to the area on gel's top surface where it contacts with the indenter. The boundary conditions are described in Figure 3, which only allow the top surface of the gel to flex during indentation. Explicit dynamic contact algorism was selected for

computational efficiency and short dynamic response time. Nlgeom setting was enabled to account for geometric nonlinearity in the simulation. As gel undergoes large deformation to maintain force equilibrium during the indentation process, causing potential nonlinearity in geometry.

Figure 3.

3. RESULTS

3.1 NHDF Contraction Force Influenced by Cell Density

Figure 4 shows the overall and corresponding single-cell contraction forces generated by fibroblasts with different cell densities. Figure 4(a) shows the total contraction forces exhibit a positively correlated increase with the cell density. Figure 4(b) shows single-cell contraction forces are similar for the low and medium seeding density of 50,000 and 100,000 cells ml^{-1}, and a noticeable, statistically significant reduction (*ca.* 26%) observed in the gels with a high cell density of 200,000 cells ml^{-1}. The results demonstrated a consistent single-cell contraction force value between the samples of two lower cell densities. Such consistency suggests that at a relatively low cell seeding density range ($\leq$ 100,000 cells ml^{-1}), all cells are sufficiently contributing to the overall contraction of the gel. This result also leads to the adaptation of 50,000 cells ml^{-1} seeding density for the study on the contractility of young and aged NHDF. The selected seeding density is also in line with the previous research on the ideal cell seeding density for the study on long-term (more than 24h) contraction force measurement [18].

Figure 4.

3.2 Contractility Difference Between Young and Aged NHDF

Figure 5 shows the level of contraction force generation by both a single young and aged NHDF within the collagen hydrogel. In the absence of TGF-β1 treatment, NHDF from young donors shown statistically significant less contractility of approximately 38% compared to those from the aged donors. However, under TGF-β1 (5 ng ml^{-1}) stimulations, higher response to the agonist treatments have shown by young NHDF, reflected in the significant increase in contraction force. The single-cell contraction force by the TGF-β1 treated young NHDF has shown an increase of 78% while aged counterparts did not significantly change.

Figure 5

Figure 6 shows the Young's moduli and the thickness of the sample gels of different groups after contraction. Young's moduli for the young group were observed slightly lower than those of the aged group (Figure 6(a)), although not statistically significant. Meanwhile, thicknesses of the gels are uniform across two age groups (Figure 6(b)). The lower Young's moduli of the young donor group suggest higher collagen digestion and matrix remodelling activity undergone by young NHDF. Also, a decrease in Young's moduli in the aged group under TGF-β1 treatment suggests that TGF-β1 may also stimulate collagen digestion in aged NHDF.

Figure 6.

Figure 7.

3.3 FE Parameter Analysis on Nano-indentation

We analysed the resultant stress distribution and compared the difference in the reaction force from the FE simulation and that calculated based on the Hertz contact theory. Figure 7(a) shows Von Mises stress at the indentation displacement of 0.25 mm (strain = 0.125) and the stress distributed evenly due to the axisymmetrical boundary conditions. As shown in Figure 7(b), with small displacements, the stress-strain response from FE simulation matches closely (*ca.* 5% difference) with the linear curve predicted by the Hertz contact theory. At displacements larger than 0.2 mm (strain = 0.1), the FE curve deviates away from the linearity. In the displacement range adopted in our FE analysis, the reaction force variation is less than 0.5% between the Poisson's ratio of 0.45 and 0.499, suggesting that it is suitable to model the hydrogel as an incompressible material with a Poisson's ratio of 0.5.

4. DISCUSSION

The proportionality of the total contraction force shown in Figure 4(a) demonstrated the effectiveness of the technique in measuring the contraction force of populated cells through the cell-mediated contraction of collagen hydrogel. Intuitively the single-cell contraction force measured through this technique is expected to be independent of cell density. However, sufficient anchorage of cells to the collagen fibrils by means of focal adhesion is required for traction force exertion and for sensing mechanical cues to initiate contraction. The embedded cells could saturate the available adhesion sites at high cell density, resulting in less contraction force generation. Also, as the single-cell contraction force is calculated as the total contraction force normalised by cell number (*i.e.* independent of cell density), the single-cell contraction force at the high density is lower than the others. Brightfield images (data not shown) of NHDF embedded in collagen hydrogel with different seeding densities

after contraction were used to check cells' interactions within the gels. Images show that cells had enough space to spread and separate from each other at low and medium seeding densities (50,000 and 100,000 cells ml^{-1}). However, at high density (200,000 cells ml^{-1}), cells are generally aggregated and attached with neighbouring cells. These observations support the near-equal single-cell contraction forces at low and medium densities as the interaction conditions are similar. Actin staining and confocal microscopy of embedded cells would give evidence on the number of cells that are sufficiently adhered to the matrix, contributing to the observable geometrical changes on the gel. Furthermore, among samples with high seeding density, we have observed wrinkling of the collagen hydrogels accompanied by cell escape as a result of excessive gel shrinkage.

In contrast, no such wrinkling occurred in the gels of the lower cell densities. Wrinkling and cell escape indicate a severe reduction of gel volume and cell counts within the sample gels [16]. These observations will result in discrepancies in the cell number and geometry used in force calculation.

Nevertheless, Figure 4(b) demonstrated similar results in measured forces between the low and medium cell densities. This similarity suggests that embedded cells underwent minimal proliferation during the culturing time, providing confidence in adopting initial cell seeding density in the calculation.

TGF-β1 is a cytokine associated with wound healing and ageing that can impact on dermal fibroblast function. The effect of TGF-β1 is especially prominent in fibroblast contraction as it initiates fibroblast differentiation towards a myofibroblast phenotype by inducing alpha smooth muscle actin (αSMA) expression [23]. The contractility of fibroblasts under TGF-β1

stimulation is thus an indication of the ability of fibroblasts to engage in normal skin homeostasis.

Previous studies have demonstrated the aged-related decline of fibroblast functions in various aspects related to contractility such as ECM remodelling, migration and protein synthesis, amongst others [8, 24]. Our results, shown in Figure 5(a) and (b), suggest lower basal contractility of young NHDF without agonist stimulation, which would give it a greater ability to respond to agonist before a saturation threshold is reached. Studies have suggested that various serum will stimulate fibroblast contraction [20], and in particular, FBS affects fibroblast-mediated collagen gel contraction [25]. No previous publication has yet clearly addressed how FBS will stimulate young and aged dermal fibroblasts differently nor given evidence on how its concentration relates to the ability in stimulating fibroblast contraction. The current result may suggest that aged NHDF respond more to a lower FBS level than young ones. Moreover, the higher basal contraction in the aged group indicates that the cell population is more primed towards a myofibroblasts phenotype. Such a transition could result in the reduction to their contribution towards other functions in normal skin maintenance, giving rise to some of the deteriorations observed in ageing skin [26].

The TGF-β family of molecules have been shown to mediate functional changes in ageing and disease processes [27]. The age-related changes in the expression of TGF-β and the change in the quantities and ratios of different TGF-β receptors on cells were believed to be closely related to degenerative diseases such as Osteoarthritis [28] and Alzheimer's disease [29]. TGF-β1 will increase contraction force generation by increasing the synthesis of actin, fibronectin and matrix receptors [20]. During skin ageing, the ECM undergoes progressive

deterioration and fragmentation due to reduced MMP and collagen transcription resulting from diminished TGF-β receptor expression and attenuated TGFβ-1/Smad signalling as previously shown in cultured human dermal fibroblasts [30-32]. The loss of collagen expression and degradation of ECM can impair the attachment of dermal fibroblasts within the dermis which results in a change in cellular morphology, resulting in smaller cells with less mechanical force [33]. This in turn has implications for TGF-β1 signalling, since it has been demonstrated that a reduction in fibroblast size and mechanical force can downregulate TGF-β receptor II (TGF-βRII) expression which further diminishes TGF-β1 signalling pathways [34]. The reduction in TGF-β stimulated contraction force in dermal fibroblasts from aged donors observed in our study is consistent with the literature reports on ageing-related perturbations in TGF-β receptor-mediated signalling events in the skin [35]. However, this does not address the apparent higher contraction force seen in unstimulated aged dermal fibroblast hydrogels. Such findings may suggest the lower tendency of myofibroblast transition in the NHDF population derived from young donors.

Fibroblasts undergo constant matrix remodelling involving generation and digestion of collagen within the hydrogel. The collagen concentration in the cell-embedded hydrogel can be indirectly assessed by its Young's modulus. The lower Young's moduli exhibited by gels within the young donor group suggests a lower collagen concentration. Thus, it is evident that young NHDF have shown a higher level of remodelling activities.

Comparing the corresponding gel's Young's moduli with or without the presence of TGF-β1 within each group, a trend of Young's moduli reduction can be seen in the aged group after treatment. This observation suggests that TGF-β1 may also stimulate the remodelling behaviour of aged fibroblasts, yet the remodelling activities are still less than the young

group. However, a previous study suggests that the thickness of the gel, together with the measured diameter of the hydrogel, was used to calculate its volume [18]. The slightly lower gel thickness in the aged group corresponds to the difference in the diameter after contraction between the groups, resulting in consistent gel volume across different sample groups. Comparing the gel thickness between control and TGF-β1 treated samples in each group (Figure 6(b)), a slight difference can be seen. However, the difference is small and has minimal effects in contraction force calculations. The fact that hydrogels are disk-shaped (with large diameter/thickness ratio), dislodged and suspended at the first instance after polymerisation, results in the majority of the contraction of hydrogel occurring along the diameter of the gel. In other words, gel radius reduction plays a major role in cell-mediated gel contraction rather than the thickness change. For example, the post-contraction gel thickness (h_1) observed for the treated group is 3% lower than the control group. As can be seen from equation (5), the single cell contraction force is linearly proportional to the product of the sum of gel thicknesses before and after contraction ($h_0 + h_1$) and the radius reduction ($r_0 - r_1$). The 3% difference in h_1 leads to less than a 1.5% difference in the value of the ($h_0 + h_1$), which is trivial compared to the more than 70% difference in ($r_0 - r_1$) as a result of the significant reduction of gel radius.

The simulation of nano-indentation on FE suggests that, despite the common belief that many hydrogel materials often exhibit nonlinear stress-strain responses, the indentation of the collagen hydrogel is primarily governed by linear deformation at small displacements. Thus, nano-indentation of the collagen hydrogel can be modelled as linearly elastic for a more straightforward calculation in the future. However, a further increase in the displacement will lead to a nonlinear regime of the indentation, where the material nonlinearity must be taken into consideration. The results are also in agreement with the

previous study, which showed a characteristic of nonlinear stress-strain response to higher strains in fibrous networks formed from collagen type I [36]. The results on the reaction force from FE simulation and theoretical calculation also show that the indentation speed adopted in the technique is appropriate for the collagen hydrogel, and the assumptions made (*e.g*. Poisson's ratio =0.5) in the theoretical model is valid for the determining Young's modulus of the gel used in the novel technique in measuring cell contraction force.

5. CONCLUSIONS

Our findings from experiments in cell-embedded collagen hydrogel-based contraction force measurements with different cell seeding densities indicate that 50,000 cells ml^{-1} is an optimal seeding density to achieve effective and accurate measurements on dermal fibroblasts. The results show a significantly higher basal contractility in NHDF from aged donors, while NHDF from young donors exhibited significantly elevated contraction force generation in response to TGF-β1 treatment. The diminished contraction force following TGF- β1 treatment in dermal fibroblasts from older donors suggests a decline in the overall functional capabilities consistent with the ageing process. The results also demonstrated the capability of the novel nano-biomechanical technique to accurately differentiate contractility changes between young and aged dermal fibroblasts which may represent a potential biomarker of skin ageing for developing regenerative and therapeutic strategies.

6. ACKNOWLEDGEMENTS

The authors thank Doctor Ken Mao, School of Engineering, University of Warwick, for helpful discussions and valuable suggestions during this research work. We would also like to thank Professor Giovanni Mann, School of Cardiovascular Medicine and Sciences, Faculty of Life Sciences & Medicine, King's College London, for scientific discussion and encouragement. This study was partly funded by Ageing Research at King's (ARK).

7. REFERENCE

[1] J. Tigges *et al.*, "The hallmarks of fibroblast ageing," (in English), *Mechanisms of Ageing and Development,* Review vol. 138, pp. 26-44, Jun 2014, doi: 10.1016/j.mad.2014.03.004.

[2] F. Boraldi, G. Annovi, R. Tiozzo, P. Sommer, and D. Quaglino, "Comparison of ex vivo and in vitro human fibroblast ageing models," (in English), *Mechanisms of Ageing and Development,* Article vol. 131, no. 10, pp. 625-635, Oct 2010, doi: 10.1016/j.mad.2010.08.008.

[3] E. Proksch, J. M. Brandner, and J. M. Jensen, "The skin: an indispensable barrier," (in English), *Experimental Dermatology,* Article vol. 17, no. 12, pp. 1063-1072, Dec 2008, doi: 10.1111/j.1600-0625.2008.00786.x.

[4] C. Brun, F. Jean-Louis, T. Oddos, M. Bagot, A. Bensussan, and L. Michel, "Phenotypic and functional changes in dermal primary fibroblasts isolated from intrinsically aged human skin," (in English), *Experimental Dermatology,* Article vol. 25, no. 2, pp. 113-119, Feb 2016, doi: 10.1111/exd.12874.

[5] N. Vedrenne, B. Coulomb, A. Danigo, F. Bonte, and A. Desmoulière, "The complex dialogue between (myo)fibroblasts and the extracellular matrix during skin repair processes and ageing," (in English), *Pathologie Biologie,* Article vol. 60, no. 1, pp. 20-27, Feb 2012, doi: 10.1016/j.patbio.2011.10.002.

[6] S. Parrinello, J. P. Coppe, A. Krtolica, and J. Campisi, "Stromal-epithelial interactions in aging and cancer: senescent fibroblasts alter epithelial cell differentiation," (in English), *Journal of Cell Science,* Article vol. 118, no. 3, pp. 485-496, Feb 2005, doi: 10.1242/jcs.01635.

[7] K. Cao *et al.*, "Progerin and telomere dysfunction collaborate to trigger cellular senescence in normal human fibroblasts," (in English), *Journal of Clinical Investigation,* Article vol. 121, no. 7, pp. 2833-2844, Jul 2011, doi: 10.1172/jci43578.

[8] C. Lopez-Otin, M. A. Blasco, L. Partridge, M. Serrano, and G. Kroemer, "The Hallmarks of Aging," *Cell,* vol. 153, no. 6, pp. 1194-1217, Jun 2013, doi: 10.1016/j.cell.2013.05.039.

[9] E. S. Hwang, G. Yoon, and H. T. Kang, "A comparative analysis of the cell biology of senescence and aging," *Cellular and Molecular Life Sciences,* vol. 66, no. 15, pp. 2503-2524, Aug 2009, doi: 10.1007/s00018-009-0034-2.

[10] C. Schulze *et al.*, "Stiffening of Human Skin Fibroblasts with Age," *Clinics in Plastic Surgery,* vol. 39, no. 1, pp. 9-20, Jan 2012, doi: 10.1016/j.cps.2011.09.008.

[11] B. Li and J. H. C. Wang, "Fibroblasts and myofibroblasts in wound healing: Force generation and measurement," *Journal of Tissue Viability,* vol. 20, no. 4, pp. 108-120, Nov 2011, doi: 10.1016/j.jtv.2009.11.004.

[12] M. J. Reed, N. S. Ferrara, and R. B. Vernon, "Impaired migration, integrin function, and actin cytoskeletal organization in dermal fibroblasts from a subset of aged human donors," *Mechanisms of Ageing and Development,* vol. 122, no. 11, pp. 1203-1220, Aug 2001, doi: 10.1016/s0047-6374(01)00260-3.

[13] W. J. Polacheck and C. S. Chen, "Measuring cell-generated forces: a guide to the available tools," *Nature Methods,* vol. 13, no. 5, pp. 415-423, May 2016, doi: 10.1038/nmeth.3834.

[14] S. A. Maskarinec, C. Franck, D. A. Tirrell, and G. Ravichandran, "Quantifying cellular traction forces in three dimensions," *Proceedings of the National Academy of Sciences of the United States of America,* vol. 106, no. 52, pp. 22108-22113, Dec 2009, doi: 10.1073/pnas.0904565106.

[15] J. A. Mulligan, X. Z. Feng, and S. G. Adie, "Quantitative reconstruction of time-varying 3D cell forces with traction force optical coherence microscopy," *Scientific Reports,* vol. 9, Mar 2019, Art no. 4086, doi: 10.1038/s41598-019-40608-4.

[16] E. Bell, B. Ivarsson, and C. Merrill, "Production of a tissue-like structure by contraction of collagen lattices by human-fibroblasts of different proliferative potential in vitro,"

Proceedings of the National Academy of Sciences of the United States of America, vol. 76, no. 3, pp. 1274-1278, Mar 1979, doi: 10.1073/pnas.76.3.1274.

[17] P. Delvoye, P. Wiliquet, J. L. Leveque, B. V. Nusgens, and C. M. Lapiere, "Measurement of mechanical forces generated by skin fibroblasts embedded in a 3-dimensional collagen gel," *Journal of Investigative Dermatology,* vol. 97, no. 5, pp. 898-902, Nov 1991, doi: 10.1111/1523-1747.ep12491651.

[18] T. R. Jin, L. Li, R. C. M. Siow, and K. K. Liu, "A novel collagen gel-based measurement technique for quantitation of cell contraction force," *Journal of the Royal Society Interface,* vol. 12, no. 106, May 2015, Art no. 20141365, doi: 10.1098/rsif.2014.1365.

[19] R. A. Pena, J. A. Jerdan, and B. M. Glaser, "Effects of TGF-beta neutralizing antibodies on fibroblast-induced collagen gel contraction - implications for proliferative vitreoretinopathy," *Investigative Ophthalmology & Visual Science,* vol. 35, no. 6, pp. 2804-2808, May 1994.

[20] R. Montesano and L. Orci, "Transforming growth factor beta stimulates collagen-matrix contraction by fibroblasts - implication for wound-healing," *Proceedings of the National Academy of Sciences of the United States of America,* vol. 85, no. 13, pp. 4894-4897, Jul 1988, doi: 10.1073/pnas.85.13.4894.

[21] H. Heinrich, "Ueber die Berührung fester elastischer Körper," *Journal für die reine und angewandte Mathematik,* vol. 1882, no. 92, pp. 156-171, 1882, doi: 10.1515/crll.1882.92.156.

[22] Y. Tatara, S. Shima, and J. C. Lucero, "On compression of rubber elastic sphere over a large range of displacements. 2. Comparison of theory and experiment," *Journal of Engineering Materials and Technology-Transactions of the Asme,* vol. 113, no. 3, pp. 292-295, Jul 1991, doi: 10.1115/1.2903408.

[23] A. Desmouliere, A. Geinoz, F. Gabbiani, and G. Gabbiani, "Transforming growth-factor-beta-1 induces alpha-smooth muscle actin expression in granulation-tissue myofibroblasts and in quiescent and growing cultured fibroblasts," *Journal of Cell Biology,* vol. 122, no. 1, pp. 103-111, Jul 1993, doi: 10.1083/jcb.122.1.103.

[24] T. Fujimura, M. Hotta, T. Kitahara, and Y. Takema, "Loss of contraction force in dermal fibroblasts with aging due to decreases in myosin light chain phosphorylation enzymes," *Archives of Pharmacal Research,* vol. 34, no. 6, pp. 1015-1022, Jun 2011, doi: 10.1007/s12272-011-0619-9.

[25] T. Kobayashi *et al.*, "TGF beta 1 and serum both stimulate contraction but differentially affect apoptosis in 3D collagen gels," *Respiratory Research,* vol. 6, Dec 2005, Art no. 141, doi: 10.1186/1465-9921-6-141.

[26] J. Baum and H. S. Duffy, "Fibroblasts and Myofibroblasts: What Are We Talking About?," *Journal of Cardiovascular Pharmacology,* vol. 57, no. 4, pp. 376-379, Apr 2011, doi: 10.1097/FJC.0b013e3182116e39.

[27] K. Krieglstein, K. Miyazono, P. ten Dijke, and K. Unsicker, "TGF-beta in aging and disease," *Cell and Tissue Research,* vol. 347, no. 1, pp. 5-9, Jan 2012, doi: 10.1007/s00441-011-1278-3.

[28] D. Hodgson, A. D. Rowan, F. Falciani, and C. J. Proctor, "Systems biology reveals how altered TGF beta signalling with age reduces protection against pro-inflammatory stimuli," *Plos Computational Biology,* vol. 15, no. 1, Jan 2019, Art no. e1006685, doi: 10.1371/journal.pcbi.1006685.

[29] F. Jeffrey, "Ineffective levels of transforming growth factors and their receptor account for old age being a risk factor for Alzheimer's disease," *Alzheimer's & Dementia: Translational Research & Clinical Interventions,* vol. 5, pp. 899-905, 2019, doi: 10.1016/j.trci.2019.11.007.

[30] J. E. Mogford, N. Tawil, A. Chen, D. Gies, Y. P. Xia, and T. A. Mustoe, "Effect of age and hypoxia on TGF beta 1 receptor expression and signal transduction in human dermal fibroblasts: Impact on cell migration," *Journal of Cellular Physiology,* vol. 190, no. 2, pp. 259-265, Feb 2002, doi: 10.1002/jcp.10060.

[31] Y. I. Kim, Y. S. Kim, H. J. Ahn, I. H. Kang, and M. K. Shin, "Reduced matrix metalloproteinase and collagen transcription mediated by the TGF-beta/Smad pathway in passaged normal human dermal fibroblasts," *Journal of Cosmetic Dermatology,* vol. 19, no. 5, pp. 1211-1218, May 2020, doi: 10.1111/jocd.13114.

[32] J. Feru *et al.*, "Aging decreases collagen IV expression in vivo in the dermo-epidermal junction and in vitro in dermal fibroblasts: possible involvement of TGF-beta 1," *European Journal of Dermatology,* vol. 26, no. 4, pp. 350-360, Jul-Aug 2016, doi: 10.1684/ejd.2016.2782.

[33] J. Varani *et al.*, "Decreased collagen production in chronologically aged skin - Roles of age-dependent alteration in fibroblast function and defective mechanical stimulation," *American Journal of Pathology,* vol. 168, no. 6, pp. 1861-1868, Jun 2006, doi: 10.2353/ajpath.2006.051302.

[34] G. J. Fisher *et al.*, "Reduction of fibroblast size/mechanical force down-regulates TGF-beta type II receptor: implications for human skin aging," *Aging Cell,* vol. 15, no. 1, pp. 67-76, Feb 2016, doi: 10.1111/acel.12410.

[35] J. W. Shin *et al.*, "Molecular Mechanisms of Dermal Aging and Antiaging Approaches," *International Journal of Molecular Sciences,* vol. 20, no. 9, May 2019, Art no. 2126, doi: 10.3390/ijms20092126.

[36] S. Munster, L. M. Jawerth, B. A. Leslie, J. I. Weitz, B. Fabry, and D. A. Weitz, "Strain history dependence of the nonlinear stress response of fibrin and collagen networks," *Proceedings of the National Academy of Sciences of the United States of America,* vol. 110, no. 30, pp. 12197-12202, Jul 2013, doi: 10.1073/pnas.1222787110.

List of figure legends

Figure 1. (a) Schematic (not to scale) and (b) image of the bio-nano-indentation tester to measure Young's modulus of the cell embedded collagen hydrogel.

Figure 2. (a) Image demonstrating the experimental setup to obtain diameters of the gel samples. (b) and (c), sample images before and after cell contraction with the edge of the gel marked with dashed lines.

Figure 3. Details of the finite-element mesh of collagen hydrogel for simulations of nano-indentation. The hydrogel is modelled as a disk such that the entire model has rotational symmetry around the left boundary of the mesh. Encastre boundary condition is applied to the bottom surface of the gel. The indentation is applied at the top-left corner of the construct downwards in a vertical direction.

Figure 4. Contraction forces generated without TGF- β1 treatment at 10% FBS for three different cell densities (a) total contraction forces (b) single-cell contraction forces. Data denote mean ± SEM, n = 3 donors, *P < 0.05 (one-way ANOVA with Tukeys post-hoc test).

Figure 5. (a) Single-cell contraction force of NHDF from donors of different age with/without TGF- β1 treatment. (b) single-cell contraction force of NHDF grouped by donor age. Data denote mean ± SEM, n = 3 donors, *P < 0.05, **P < 0.001 (two-way ANOVA with Tukeys post-hoc test).

Figure 6. Post-contraction hydrogel parameters grouped by donor age. (a) Young's moduli. (b) Thickness. Data denote mean ± SEM, n = 3.

Figure 7. Results from finite element simulation of nano-indentation of collagen hydrogel with cylindrical glass indenter. (a) The distribution of Von Mises stress in hydrogel at indentation displacement 0.25 mm (b) The comparison of force-displacement curves between finite-element simulation (Poisson's ratio = 0.499) and the Hertz contact theory.

CRediT author statement

Zhuonan Yu: Methodology; Software; Validation; Formal analysis; investigation; Data curation; Writing- Original draft preparation

Matthew J. Smith: Methodology; Formal analysis; Writing- Review & Editing; Visualization

Richard C. M. Siow: Writing- Review & Editing; Funding acquisition

Kuo-Kang Liu: Supervision, Validation, Writing- Reviewing & Editing.

Declaration of competing interest

The authors declare that they have no known competing financial interests or personal relationships that could have appeared to influence the work reported in this paper.

Highlights

- Aged human dermal fibroblasts are more contractile than young cells.
- Young cells are more responsive to stimulation of transforming growth factor β1.
- Contractility change of dermal fibroblasts may be used as a biomarker for ageing.
- Nanobiomechanical tester enables cell-friendly quantification in contractility.
- Finite element simulations gauge a measurement range for theoretical analyses.

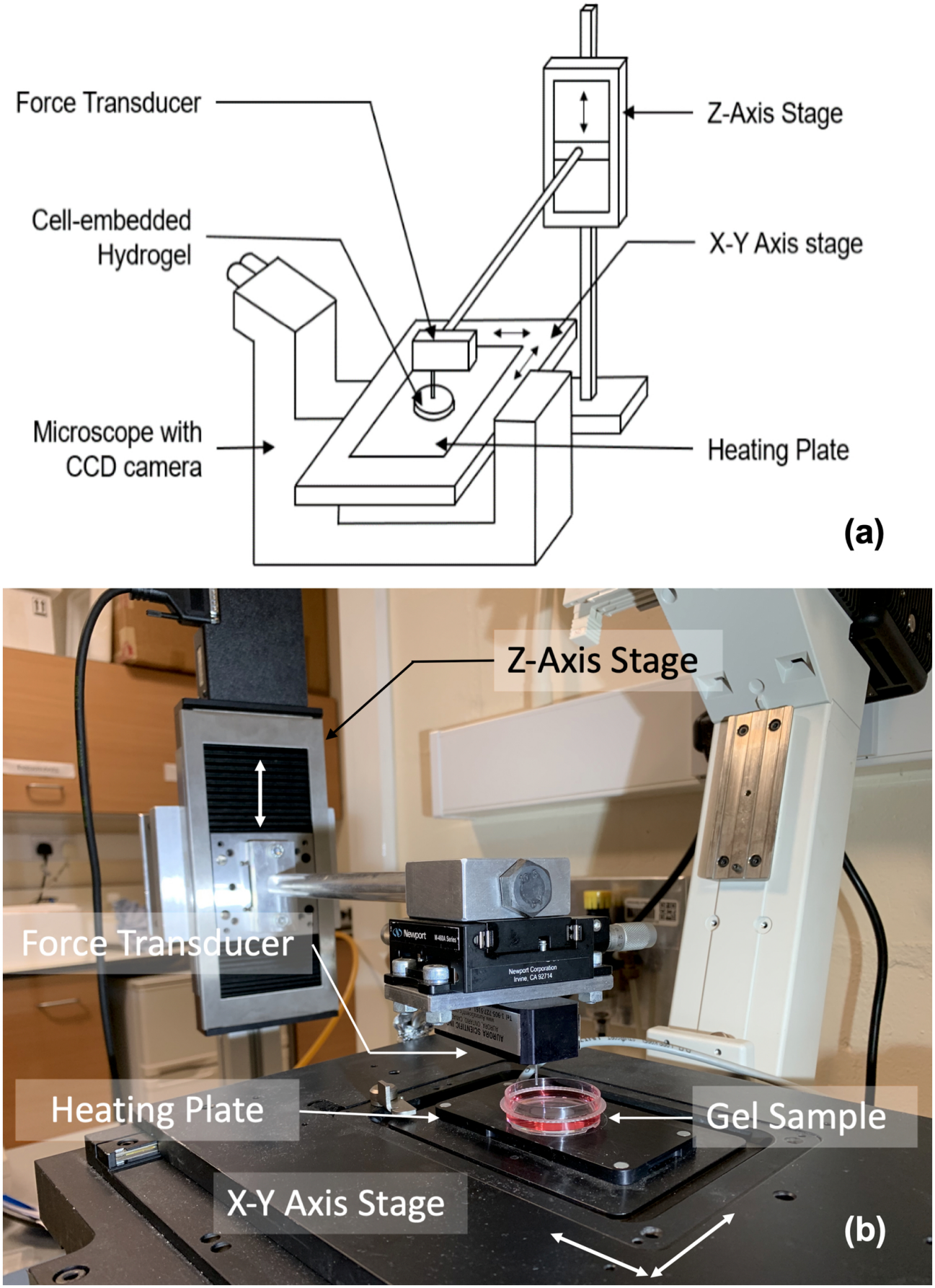
Force Transducer
Z-Axis Stage
Cell-embedded Hydrogel
X-Y Axis stage
Microscope with CCD camera
Heating Plate
(a)
Z-Axis Stage
Force Transducer
Heating Plate
Gel Sample
X-Y Axis Stage
(b)

Figure 1

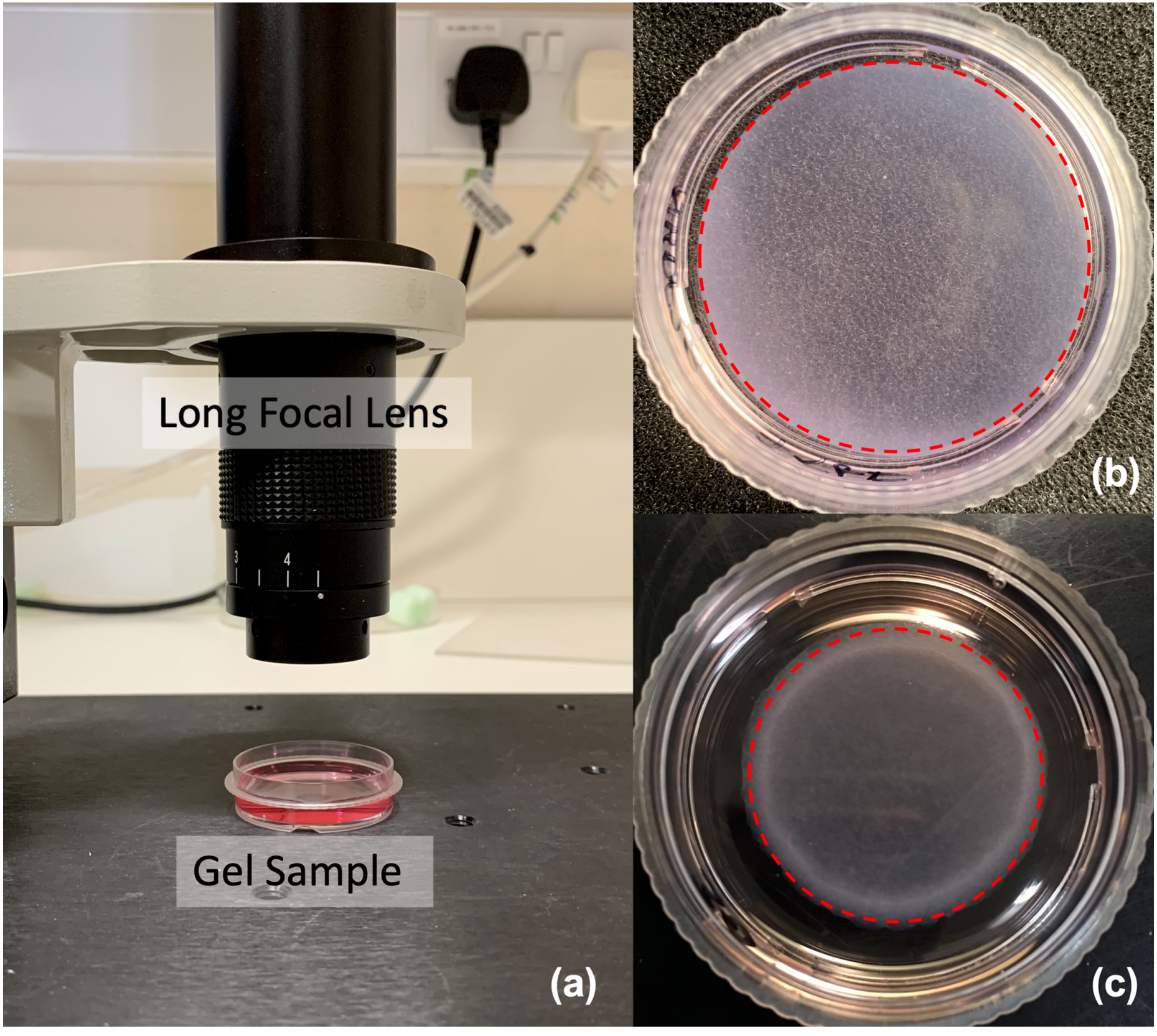

Figure 2

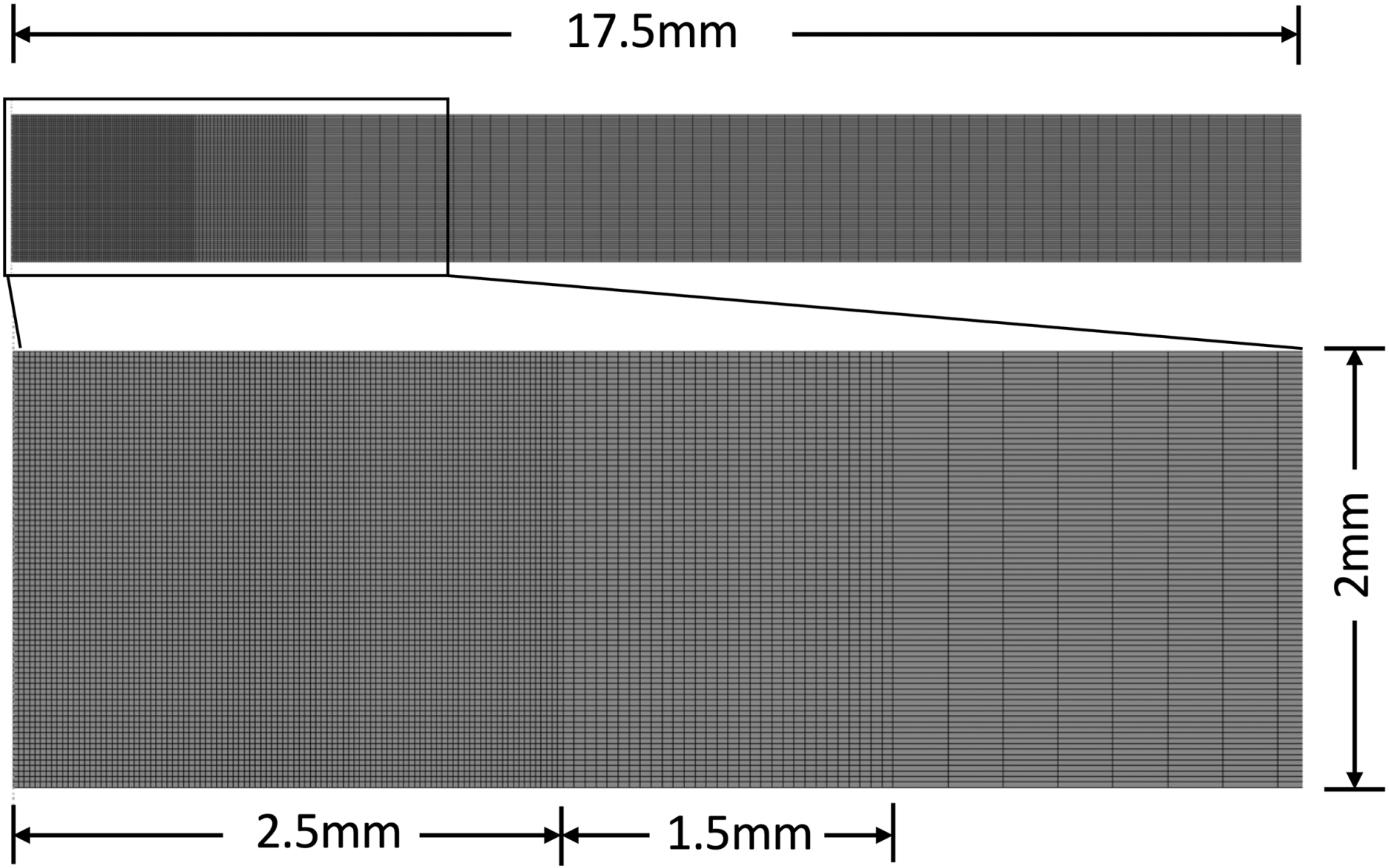

Figure 3

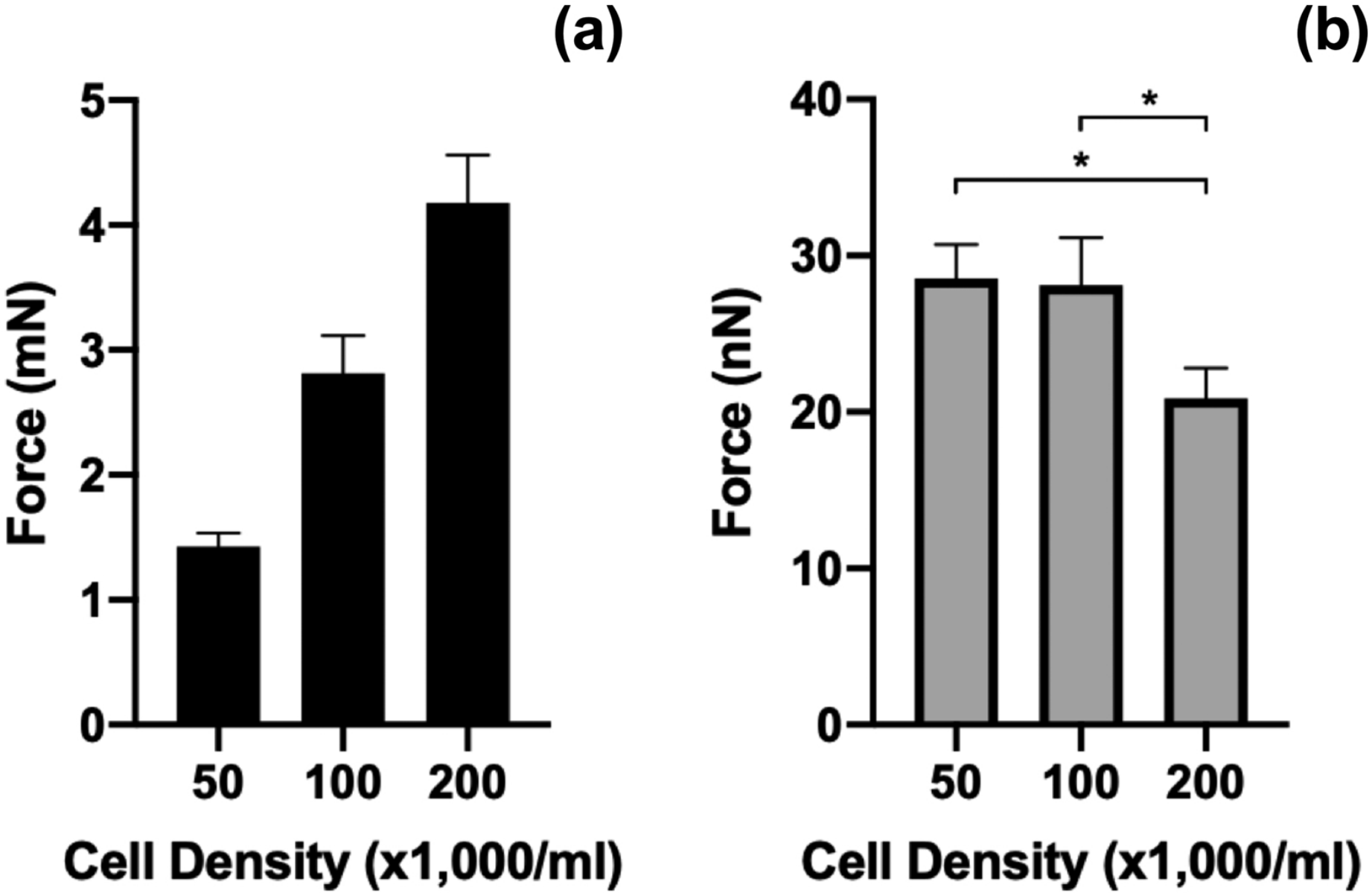
(a)
Force (mN)
5
4
3
2
1
0
50
100
200
Cell Density (x1,000/ml)
(b)
Force (nN)
40
30
20
10
0
*
*
50
100
200
Cell Density (x1,000/ml)

Figure 4

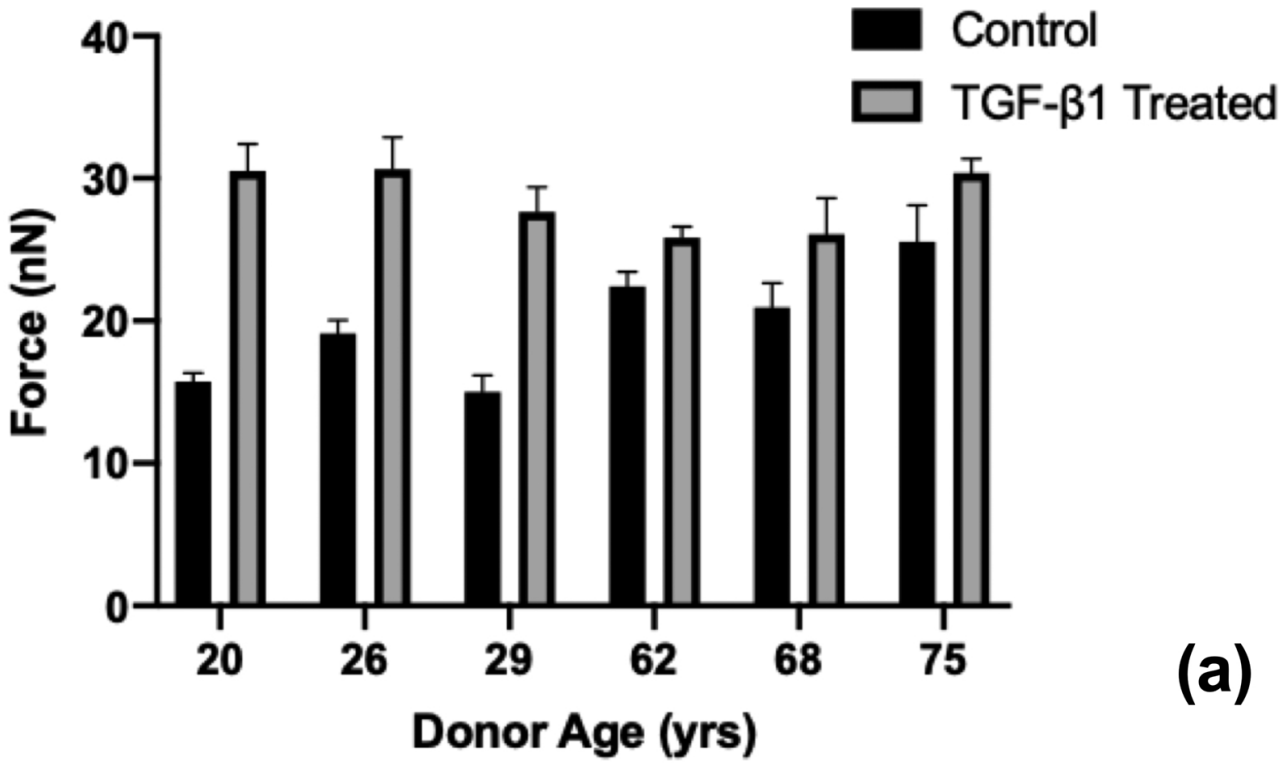
Control
TGF-β1 Treated
Force (nN)
40
30
20
10
0
20
26
29
62
68
75
Donor Age (yrs)

(a)

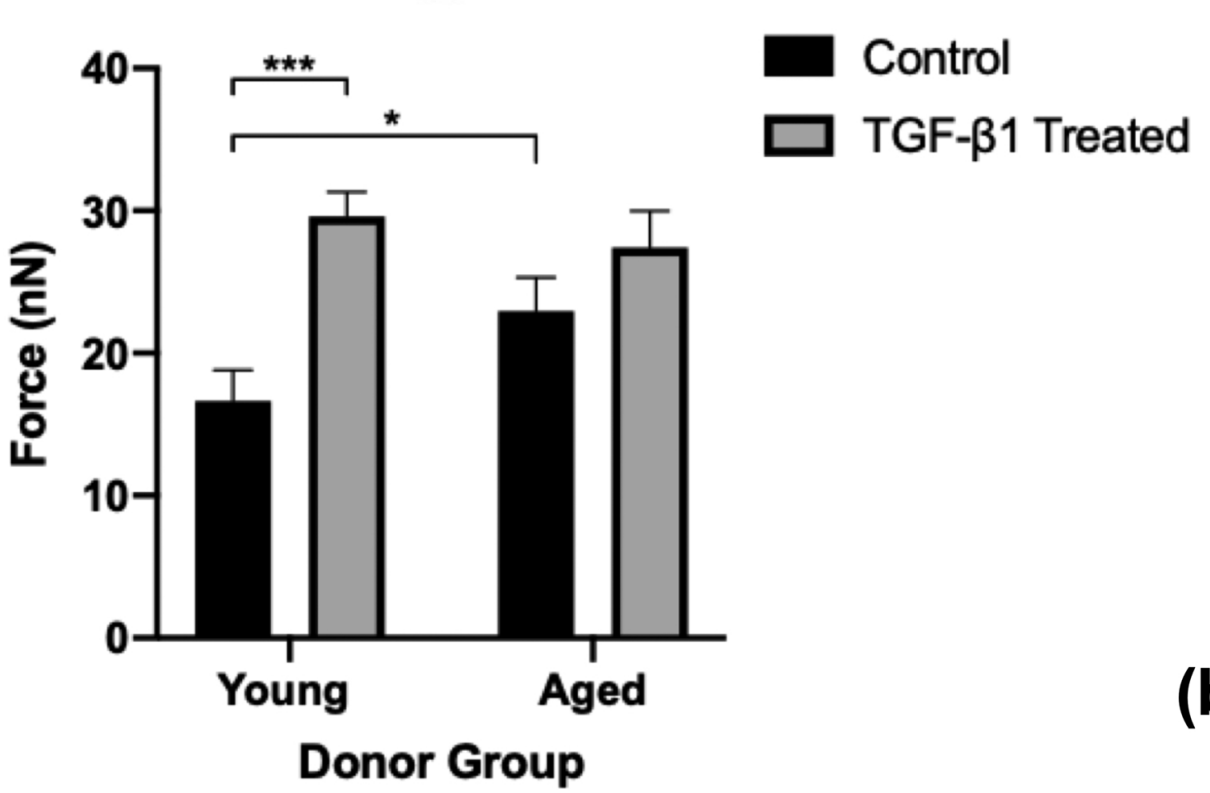
Control
TGF-β1 Treated
***
*
Force (nN)
40
30
20
10
0
Young
Aged
Donor Group

(b)

Figure 5

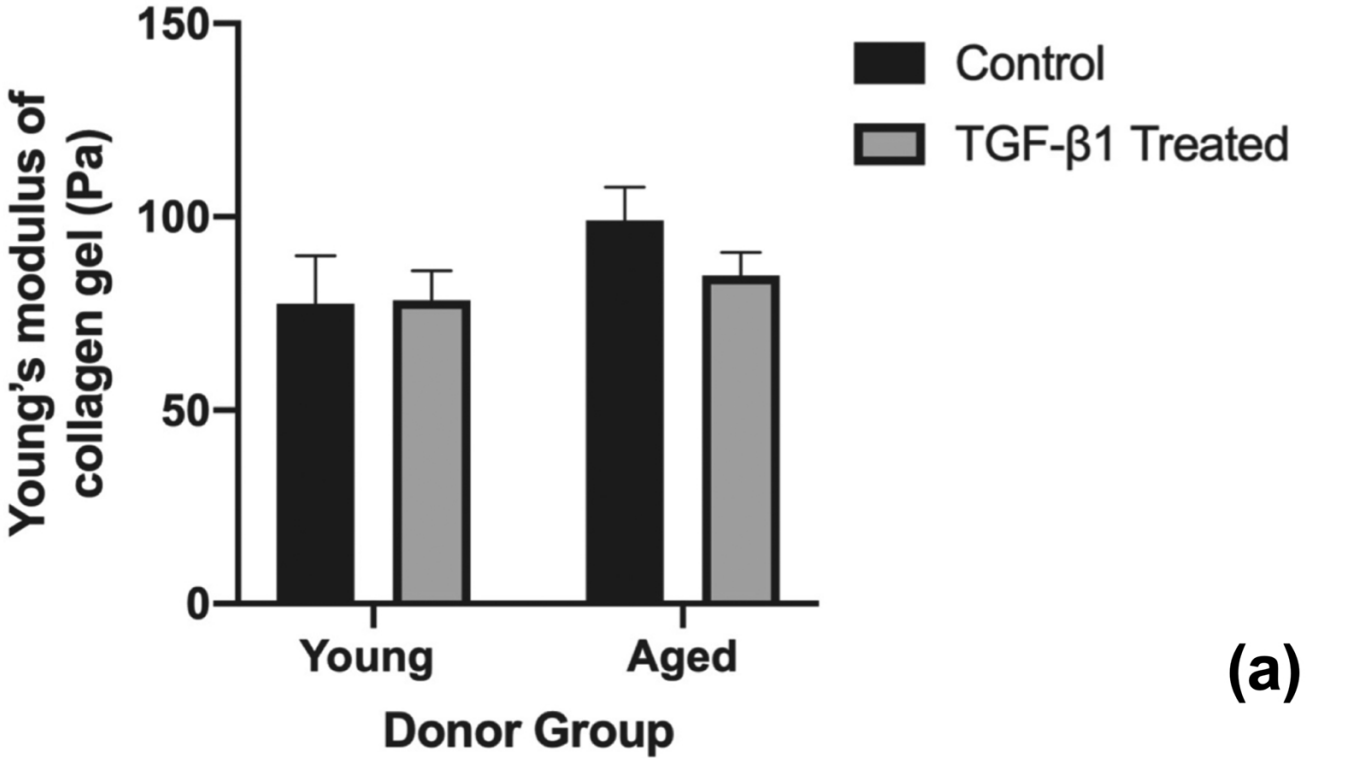
150
100
50
0
Young's modulus of collagen gel (Pa)
Control
TGF-β1 Treated
Young
Aged
Donor Group
(a)

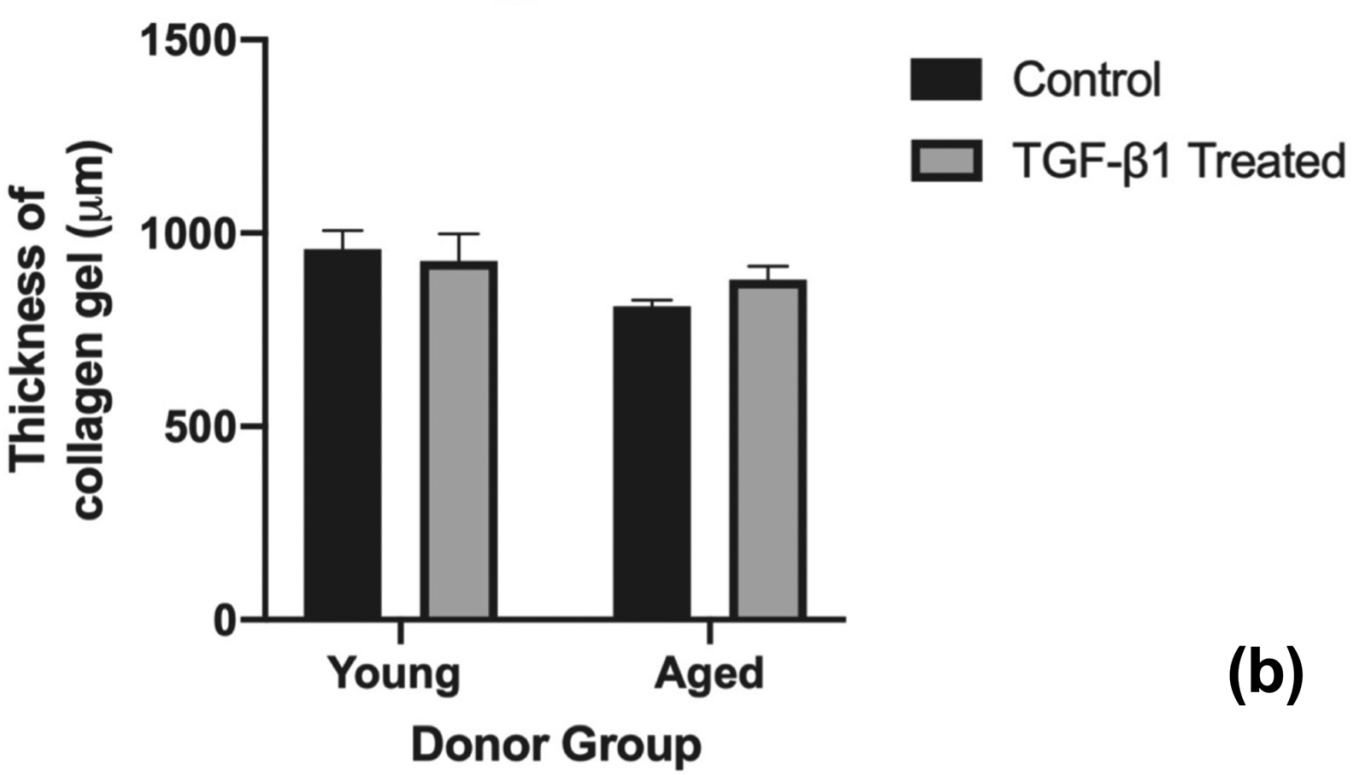
1500
1000
500
0
Thickness of collagen gel (μm)
Control
TGF-β1 Treated
Young
Aged
Donor Group
(b)

Figure 6

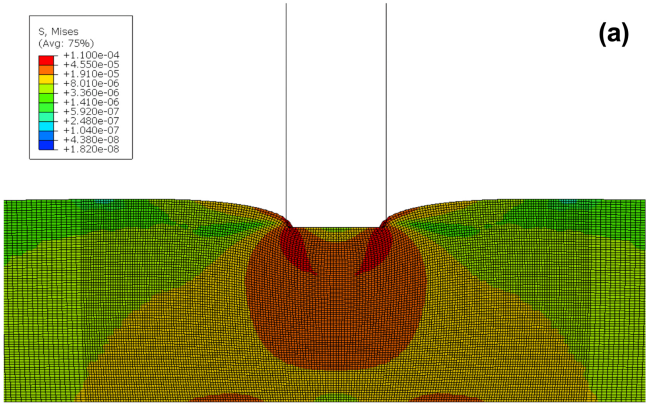
S, Mises
(Avg: 75%)
+1.100e-04
+4.550e-05
+1.910e-05
+8.010e-06
+3.360e-06
+1.410e-06
+5.920e-07
+2.480e-07
+1.040e-07
+4.380e-08
+1.820e-08
(a)

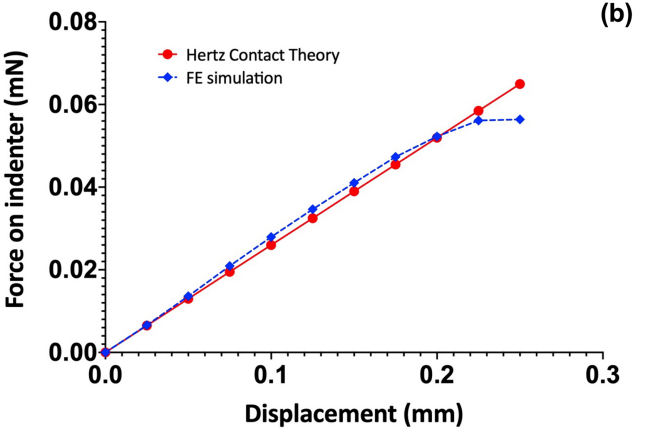
(b)
Hertz Contact Theory
FE simulation
Force on indenter (mN)
0.08
0.06
0.04
0.02
0.00
0.0
0.1
0.2
0.3
Displacement (mm)

Figure 7